Hydration of Tricalcium and Dicalcium Silicate Mixtures Studied Using Quasielastic Neutron Scattering

Vanessa K. Peterson,*,†,‡ Dan A. Neumann,† and Richard A. Livingston§

Center for Neutron Research, National Institute of Standards and Technology, Gaithersburg, Maryland 20899-8562, Department of Materials Science and Engineering, University of Maryland, College Park, Maryland 20742-2115, and Federal Highway Administration, HRDI-05 McLean, Virginia 22101

Received: April 25, 2005; In Final Form: June 3, 2005

Quasielastic neutron scattering was used to study the hydration reaction of tricalcium and dicalcium silicate mixtures by following the fixation of hydrogen into the reaction products, and by applying hydration models to the data. The reaction kinetics were well-described by an Avrami-derived model for the nucleation and growth regime during early hydration times and a diffusion-limited model for later periods. This study showed that the hydration reaction is not a simple linear combination of the reactions for the individual components. Compressive strength tests correlated with the neutron scattering data, suggesting that the details of the interaction affect the microstructure and therefore the strength of the product. Results suggest that favorable reaction mechanics provide optimal strength when an 80−95% tricalcium silicate and 20−5% dicalcium silicate mixture is used.

1. Introduction

Cement, the most widely used construction material in the world, is predominantly a complex calcium silicate mixture that reacts with water to produce a material with desirable mechanical properties. Although the hydration of Portland cement is a complex process involving several simultaneous chemical reactions, tricalcium silicate is the component responsible for early strength development in cement, and its hydration mechanics have been investigated for many years, using a variety of techniques. It has, however, long been recognized that the hydration of cement involves the *interaction* of the many different components. Despite this, very few controlled studies of the combined reactions of tricalcium and the other calcium silicate phase, dicalcium silicate, have been undertaken. Tong and Young investigated the ionic products (K_{ip}) of $Ca(OH)_2$ over the course of the first week of reaction of mixtures of dicalcium silicate with 5 and 10 wt % tricalcium additions, and compared these mixtures to pure tricalcium silicate and dicalcium silicate pastes.[1] They found that even at these small amounts, the presence of tricalcium silicate restores the high degree of supersaturation with respect to $Ca(OH)_2$ that would normally be observed in pure tricalcium silicate. Odler and Schüppstuhl found that the rate of dicalcium silicate hydration was accelerated significantly by the presence of tricalcium silicate.[2] They also reported that the kinetics of the tricalcium silicate phase in the mixture remained essentially unaltered by the presence of the dicalcium silicate phase, up to a 50:50 mixture.

Here we report a detailed quasielastic neutron scattering study of the reaction of carefully controlled mixtures of synthetic tricalcium and dicalcium silicate. Identical mixtures were also prepared and their 28-day compressive strength was measured and correlated with the quasielastic neutron scattering results.

* Corresponding author. E-mail: vanessa.peterson@nist.gov (V. Peterson).
† National Institute of Standards and Technology, Gaithersburg.
‡ University of Maryland.
§ Federal Highway Administration.

2. Background

2.1. Hydration of Tricalcium and Dicalcium Silicate. Tricalcium silicate is the most important and abundant component of Portland cement clinker, comprising 50−70 wt % of the total components. It reacts quickly with water and is the most important component for strength development, particularly in the first 28 days.[3] The hydration of tricalcium silicate is typically written

$$2Ca_3SiO_5 + 7H_2O \rightarrow 3CaO{\cdot}2SiO_2{\cdot}4H_2O + 3Ca(OH)_2 + 173.6\text{kJ} \quad (1)$$

Dicalcium silicate is the second most abundant component, comprising 15−30 wt % of clinker. Dicalcium silicate reacts slowly, contributing little to the strength development in cement at ages less than 28 days. It does, however, contribute substantially to the strength development beyond that time. The hydration of dicalcium silicate is

$$2Ca_2SiO_4 + 5H_2O \rightarrow 3CaO{\cdot}2SiO_2{\cdot}4H_2O + Ca(OH)_2 + 58.6\text{ kJ} \quad (2)$$

It has been shown that in a cement paste at 28 days, about 70% of the total tricalcium silicate, and about 30% of the total dicalcium silicate, have reacted.[3] Compressive strength development is believed to run parallel to the course of the chemical reactions for the hydration of these two phases. Industrially, ordinary Portland cement clinkers typically contain a tricalcium silicate:dicalcium silicate ratio of 3:1.[3]

The hydration reaction for the more reactive tricalcium silicate can be divided into three sections: initial hydrolysis, nucleation and growth, and diffusion-limited hydration. Initial hydrolysis is the irreversible dissolution of the outer tricalcium silicate grain. This initial hydrolysis period when the tricalcium silicate grains rapidly release calcium and hydroxide ions, and a large amount of heat, is short, quickly slowing. The nucleation and growth period begins with the formation of calcium silicate

10.1021/jp052147o CCC: $30.25
Published on Web 07/08/2005

hydrate (C−S−H) and $Ca(OH)_2$. As the C−S−H layer thickens around the unreacted tricalcium silicate grains, it becomes increasingly difficult for water molecules to reach the unhydrated tricalcium silicate. The speed of the reaction is now controlled by the rate at which water molecules diffuse through the C−S−H, known as diffusion-limited hydration. This coating thickens over time causing the production of C−S−H to slow. The hydration will continue as long as water and tricalcium silicate are present.

Dicalcium silicate reacts with water in a similar manner compared to tricalcium silicate, but much more slowly, and with less heat evolved. The products from the hydration of dicalcium silicate are the same as those for tricalcium silicate.

2.2. Application of Quasielastic Neutron Scattering. The essential step in the hydration of cement components is the transfer of protons from the free water to the solid, and then to the various products that form. Thus, one can follow the hydration reaction by determining the state of hydrogen as the reaction progresses. As a result of the high sensitivity of neutrons for hydrogen, Quasielastic Neutron Scattering (QENS) provides a direct measure of the conversion of free water to structurally/chemically bound water and to water constrained in the pores of the cement paste. In this way, the mechanics of hydration can be probed using the QENS spectra, $S(Q,\omega)$, which represent the incoherent scattering from hydrogen (S) as a function of scattering vector (Q) and energy change (ω).[4−8]

3. Experimental Section

3.1. Sample Preparation. Triclinic phase pure T_1-type tricalcium silicate and monoclinic phase pure β-type dicalcium silicate powders were obtained from Construction Technology Laboratories (CTL, Skokie, IL). Particle size analysis was conducted by CTL, using an average of four measurements to determine the average particle size and specific surface area of dicalcium silicate to be 21 μm and 0.082 $m^2\ g^{-1}$, respectively, and of tricalcium silicate to be 9.8 μm and 0.533 $m^2\ g^{-1}$. Each individual sample, as well as mixtures of the two, were hydrated by using distilled water and a water:cement ratio of 0.4. The composition of each mixture was defined by using the mass ratio of tricalcium silicate to total mixture, x. Typical error in x was 5×10^{-4}.

3.2. Compressive Strength Testing. One cubic inch mortars of each mixture were prepared by using C778 graded standard sand from the National Institute of Standards and Technology (NIST). Samples were cured at 30 °C, and contained a cement:water:sand mass ratio of 1:0.4:2.75, in accordance with the ASTM C 109 standard, which was followed for the testing.[9] Three duplicates of each sample were prepared and tested. Prior to sample testing, an ordinary Portland cement (OPC) test set of mortars was prepared with cement MA-146 from NIST.

3.3. QENS Measurement. QENS measurements were carried out with the NIST Fermi chopper time-of-flight neutron spectrometer.[10] Hydration took place inside a Teflon bag inside a rectangular aluminum hydration cell, at 30 °C. The sample thicknesses were approximately 1 mm in the hydration cell, which was placed at a 45° angle to the incident neutron beam, in reflection geometry. Data from only the higher angle detectors facing the sample face of the cell from 95.2° to 135.5° were used. QENS measurements were commenced 30 min after initial mixing, and the results were time-averaged in 33-min slices. Data were collected continuously up to 55 h.

The incident neutron wavelength used was 4.8 Å and the sample-to-detector distance was 2.29 m. The calculated elastic scattering energy resolution, ΔE, was 0.146 meV. Data were summed from several detectors corresponding to the Q range of 2.0−2.3 $Å^{-1}$.

TABLE 1: Typical Peak Fitting Parameters Derived from PAN Fitting to QENS Data of a 50:50 Mixture of Tricalcium and Dicalcium Silicate[a]

derived integrated area	full width at half max
C (bound H)	$W_C = 0.146$ (fixed)
P (pseudobound H)	$W_P = 0.4(1)$
F_1 (free H)	$W_{F_1} = 1.22(3)$
F_2 (free H)	$W_{F_2} = 10.5(2)$

[a] Errors are absolute.

3.4. Analyses and Modeling of QENS Data. The profile utility PAN within the Data Analysis and Visualization Environment (DAVE)[11] was used for the analyses of QENS data. The QENS spectra were modeled with four components:

1. An elastic peak representing completely bound hydrogen was modeled by using a resolution-limited Gaussian line shape of width W_C and integrated area C.

2. The narrowest quasielastic-broadened component arising from pseudobound hydrogen was modeled by using a Lorentzian line shape of width W_P and integrated area P.

3. A wider quasielastic-broadened component, also arising from hydrogen in the "free" water, was modeled by using a Lorentzian line shape of width W_{F_1}.

4. A very broad quasielastic-broadened component arising from hydrogen in the "free" water was modeled by using a Lorentzian line shape of width W_{F_2}.

The profile used to describe the resolution of the Fermi chopper spectrometer has been shown to be a Gaussian function.[8] As the line widths for the Lorentzian components were much greater than the resolution function, they were not convolved with the resolution function. The method used follows:

$$S(Q,\omega) = \frac{C}{\sqrt{2\pi(W_C/2.354)^2}} e^{-(1/2)((\hbar\omega-(\hbar\omega)_0)/(W_C/2.354))^2} + \frac{W_P}{2\pi}\frac{P}{(\hbar\omega-(\hbar\omega)_0)^2+(W_P/2)^2} + \frac{W_{F_1}}{2\pi}\frac{F_1}{(\hbar\omega-(\hbar\omega)_0)^2+(W_{F_1}/2)^2} + \frac{W_{F_2}}{2\pi}\frac{F_2}{(\hbar\omega-(\hbar\omega)_0)^2+(W_{F_2}/2)^2} \quad (3)$$

In the above, $\hbar\omega$ is the energy and $(\hbar\omega)_0$ (which remained approximately 0) is the center for each peak. In all calculations, $(\hbar\omega)_0$ was constrained to be the same for each component. W_{F_1} and W_{F_2} were determined from data for the first seven time-averaged slices (3.85 h), where all the water was assumed to be in the free state, and the value was fixed for subsequent fits. For this determination, an elastic line was included to account for contributions from the unreacted tricalcium silicate grains, and the sample cell. In a similar manner, W_P was determined from the final seven time-averaged slices of reaction time, and the one Gaussian and three Lorentzian components were used in this determination. W_C was fixed to the instrument resolution at the elastic line. The average W_P determined from these last seven spectra was fixed for fits at previous reaction times. Thus, the five variables that were used in the profile fitting were $(\hbar\omega)_0$, and the four integrated areas C, P, F_1, and F_2 (see Table 1).

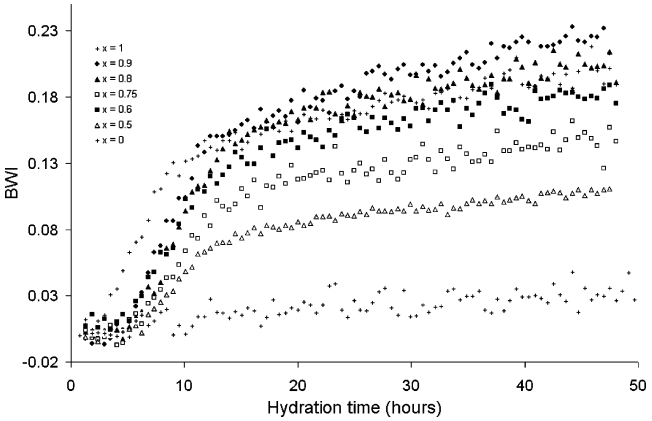

Figure 1. Variation of the BWI over a 50 h period during the hydration of tricalcium and dicalcium silicate mixtures, where x = mass ratio of tricalcium silicate to total mixture. For clarity, only a selection of the hydration curves are included, and error bars are omitted.

The Bound Water Index (BWI) is defined[5]

$$\mathrm{BWI} = 1 - \mathrm{FWI} = \frac{C + P}{C + P + (F_1 + F_2)} \qquad (4)$$

With use of the BWI, the nucleation and growth, and diffusion limited hydration regimes were modeled by using eqs 5 and 6, which have previously been applied to tricalcium silicate hydration.[4]

$$\mathrm{BWI}(t) = \mathrm{BWI}(0) + A[1 - \exp\{-[k(t - t_\mathrm{i})]^n\}] \qquad (t_\mathrm{i} \le t \le t_\mathrm{d}) \quad (5)$$

$$\mathrm{BWI}(t) = \mathrm{BWI}(0) + [1 - \{[1 - \mathrm{BWI}(t_\mathrm{d})]^{1/3} - (R^{-1})(2D_\mathrm{i})^{1/2}(t - t_\mathrm{d})^{1/2}\}^3] \qquad (t > t_\mathrm{d}) \quad (6)$$

In the above equations, BWI(t_d) is the bound water index predicted at the time that diffusion-limited kinetics begin, t_d, and BWI(0) was taken as the BWI at time t_i. R^{-1} is the mean inverse radius of the initial unhydrated particle size. D_i is an effective diffusion coefficient, k is the nucleation and growth reaction rate constant, and A is the BWI after infinite time. The exponent n has been determined experimentally to be 2.65 at 30 °C for tricalcium silicate, and this value was used to model QENS data for all mixtures.[12] R^{-1} was determined from particle size distribution reports sent from CTL. For the mixtures, the R^{-1} corresponding to the dominant phase of the mixture was used. t_i was established from the QENS hydration plots of t versus BWI(t). t_d was also established from these curves, from the narrow range that resulted in the smooth transition from nucleation and growth to diffusion-limited kinetics in the model. The free parameters in the model were D_i, A, and k, which were fitted to the data in the hydration curves.

4. Results and Discussion

4.1. QENS Data Analyses and Modeling. BWI results for the hydration of the mixtures, as derived from the QENS data, are shown in Figure 1. For clarity, error bars have been omitted from this figure.

Typical absolute error in a BWI curve is shown in Figure 2, which features an insert detailing a typical fitting in PAN. It is clear from this that the reaction at intermediate compositions cannot be simply described as a linear combination of the end points. While the BWI hydration curves are directly useful for qualitative comparison, quantitative differences between the hydration of similar mixtures are more easily interpreted with the aid of the hydration models.

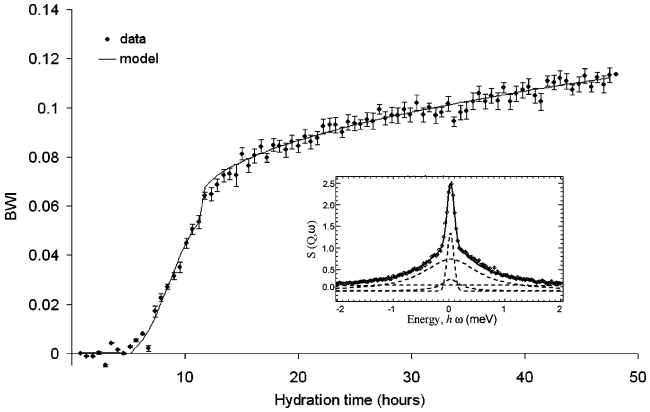

Figure 2. Typical fitting of the diffusion models to the BWI derived from the QENS data for a mixture with a tricalcium silicate: total tricalcium and dicalcium silicate ratio of 0.5 (x = 0.5). Error bars represent absolute error. The insert shows a snapshot from the PAN fitting for the QENS data for the sample at 5 h hydration time, detailing the Gaussian and three Lorentzian profiles as dotted lines. The overall fit is indicated by the solid line.

Figure 2 shows the BWI and fit of the model for the hydration reaction of the 50:50 tricalcium:dicalcium silicate mixture (mixture ratio of 0.5). Other curves displayed similar features, except for the dicalcium silicate curve, where the reaction was very slow, and the nucleation and growth regime was unable to be separated from the diffusion-limited regime. As expected, mixtures with a very low tricalcium-to-dicalcium silicate ratio reacted more slowly.

Table 2 lists the kinetic parameters describing the reaction, including those taken directly from the BWI results (t_i, t_d, and d(BWI)/dt)) and those derived from the hydration modeling (A, k, and D_i), for various mixtures of tricalcium and dicalcium silicate.

4.2. Discussion of the Parameters Describing the Reaction Kinetics. Figure 3 shows the variation of t_i and t_d with the ratio of tricalcium silicate in the mixture. As expected, t_i steadily decreased as the amount of tricalcium silicate, which is more reactive than dicalcium silicate, increased. This indicates that t_i was independent of the effect that the *interactions* of the mixture components had on the other derived parameters. Similarly, t_d decreased with increasing tricalcium silicate content; however, the increase was more marked from mixture ratios of 0.85−1.0. This result indicated a rapid decrease in the length of the nucleation and growth period in mixtures with a composition ratio greater than this.

The variation of A and D_i with mixture composition is shown in Figure 4. Parameter A represents the expected amount of product at infinite time, and shows a maximum for tricalcium: dicalcium silicate ratios of approximately 0.8−0.95, before decreasing. The trend of D_i correlates well with that observed for the parameter A, exhibiting a maximum for ratios of 0.8−0.95, before decreasing. D_i is greatly affected by the permeability of the C−S−H.[13] Thus, the higher D_i observed for this ratio range indicates that a more permeable C−S−H layer has formed for these compositions than for the tricalcium silicate alone, or for mixtures with less tricalcium silicate. Hence, the reaction products formed during the nucleation and growth regime differed for mixtures within the tricalcium silicate mixture ratio 0.8−0.95.

Equation 5 indicates that the rate of change of bound water, d(BWI)/dt, should be a nonlinear function of time. However,

TABLE 2: Model Parameters Derived for Hydrated Tricalcium and Dicalcium Silicate Mixtures[a]

x	A	k (h^{-1})	D_i ($m^2 h^{-1}$)	t_d (h)	t_i (h)	d(BWI)/dt
0.0000			$1.5(2) \times 10^{-18}$			
0.1500(4)	0.039(1)	0.186(3)	$3.6(4) \times 10^{-18}$	12.85(8)	5.15(8)	0.00500(7)
0.3005(4)	0.040(1)	0.219(4)	$4.3(5) \times 10^{-18}$	12.30(8)	5.70(8)	0.0075(1)
0.5000(4)	0.058(2)	0.203(4)	$8(1) \times 10^{-17}$	11.20(8)	4.05(8)	0.0087(1)
0.6003(4)	0.104(3)	0.228(4)	$2.8(3) \times 10^{-16}$	11.75(8)	4.05(8)	0.0143(2)
0.6996(4)	0.098(3)	0.224(4)	$2.5(3) \times 10^{-16}$	11.20(8)	4.05(8)	0.0163(2)
0.7499(4)	0.079(2)	0.184(3)	$2.2(3) \times 10^{-16}$	11.20(8)	3.50(8)	0.0106(1)
0.7797(4)	0.132(4)	0.126(2)	$3.6(4) \times 10^{-16}$	11.20(8)	2.95(8)	0.01400(2)
0.7996(4)	0.160(4)	0.131(2)	$4.7(6) \times 10^{-16}$	11.20(8)	2.95(8)	0.0181(2)
0.7997(4)	0.121(3)	0.166(3)	$5.0(6) \times 10^{-16}$	11.20(8)	2.95(8)	0.0186(2)
0.8995(4)	0.150(4)	0.125(2)	$5.5(7) \times 10^{-16}$	10.65(8)	1.30(8)	0.0179(2)
0.9500(4)	0.145(4)	0.146(3)	$3.0(4) \times 10^{-16}$	9.00(8)	1.30(8)	0.0187(2)
1.0000	0.109(3)	0.221(4)	$3.0(4) \times 10^{-16}$	7.90(8)	1.30(8)	0.0183(2)
1.0000	0.104(3)	0.251(4)	$2.8(3) \times 10^{-16}$	8.17(8)	1.30(8)	0.0188(2)

[a] Errors are one standard deviation.

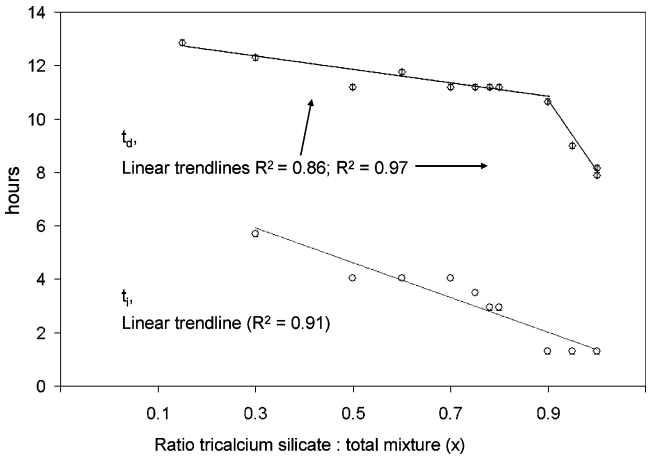

Figure 3. Variation of t_d (top) and t_i (bottom) with mixture composition of tricalcium and dicalcium silicate. Lines are linear trend lines established from a least-squares minimization, with the residuals reported inset. Error bars in y represent 1 standard deviation from the value, or are smaller than the points (as with the x axis value).

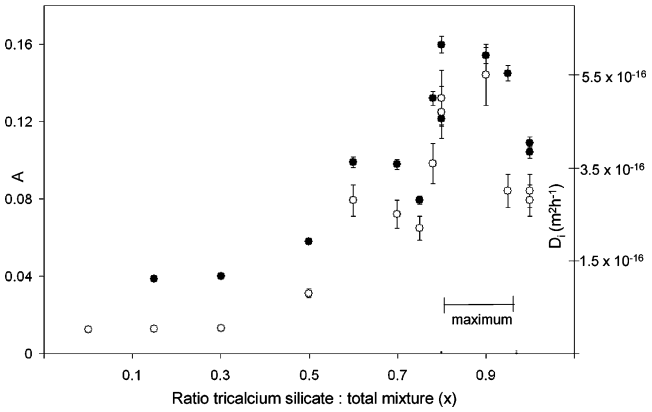

Figure 4. Variation of A (○) and D_i (●) with mixture composition of tricalcium and dicalcium silicate. The composition range yielding maximum values is highlighted inset lower right. Error bars represent 1 standard deviation from the value, and in x are smaller than the points.

the combination of kinetic parameters is such that the increase in BWI is essentially linear during the time up to the peak reaction (Figure 2). This enables d(BWI)/dt to be approximated to a constant during this period. Figure 5 is a plot of this constant value reaction rate (d(BWI)/dt) with composition ratio. In agreement with the trend observed for A and D_i, but occurring as a minimum rather than a maximum, the value for d(BWI)/dt

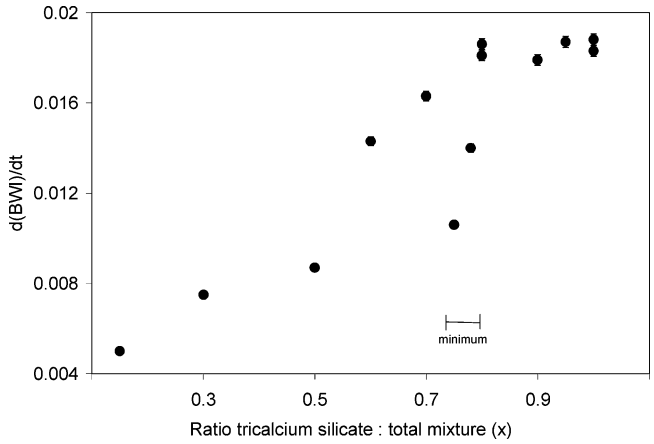

Figure 5. Variation of d(BWI)/dt during the nucleation and growth regime (linear section) with mixture composition of tricalcium and dicalcium silicate. The composition range yielding minimum values is highlighted inset lower right. Error bars in y represent 1 standard deviation from the value, or are smaller than the points (as for x values).

shows a significant decrease at the ratio 0.75 before a sharp increase to the value for pure tricalcium silicate sample.

These results indicated an interesting interaction of the dicalcium and tricalcium silicate hydration reactions. The higher rate of formation of products (d(BWI)/dt) correlates with a shorter nucleation and growth time (t_d), the appearance of a more permeable C−S−H structure (larger D_i), and ultimately more product (A). The optimal composition for these reaction kinetics occurs at tricalcium silicate ratios of 0.8−0.95.

There appeared to be a sharp transition in the rate of variation of the parameters describing the reaction kinetics, beginning at the tricalcium silicate ratio of 0.75, reaching a maximum at approximately 0.8. This dramatic rate of change is illustrated well by the parameters observed for the ratio 0.8 (Table 2). Minor variation in the composition ratio, as small as 0.0001, caused large changes to some of the parameters, for D_i, and particularly for A.

4.3. Compressive Strength. Table 3 and Figure 6 show the results for the compressive strength testing.

There were issues with the reproducibility of these tests, perhaps due to minor variation in the packing of the fresh mortars. Despite these problems, a maximum in the compressive strength was clearly observed at the ratio of 0.8. These results are therefore consistent with the observation that A, the amount of product that will ultimately form, is maximum at this ratio. We were unable to determine if the alteration to the type of product, as predicted by the sudden increase in D_i at this

TABLE 3: The 28-day Compressive Strengths of Samples (MPa)[a]

sample	average (MPa)
OPC (8 day strength)	14(1)
$x = 1.0000$ (Ca_3SiO_5)	3(1)
$x = 0.9500(4)$	6(2)
$x = 0.9000(4)$	2.8(6)
$x = 0.8000(4)$	4.0(5)
$x = 0.6000(4)$	2.2(4)
$x = 0.3000(4)$	1.8(1)
$x = 0.0000$ (Ca_2SiO_4)	1.4(2)

[a] Errors are one standard deviation.

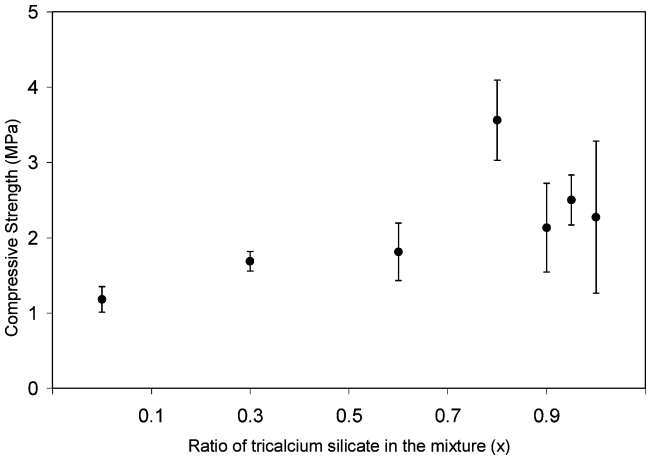

Figure 6. Average compressive strength of various tricalcium/dicalcium silicate mixtures. Error bars represent 1 standard deviation from the value, and in x are smaller than the points.

composition, was connected to the increase in strength or not. The differentiation of reaction products as C−S−H or $Ca(OH)_2$ was not attempted in this study and remains the subject for future investigations.

5. Conclusions

Quasielastic neutron scattering and compressive strength testing were used to investigate the hydration reaction of dicalcium and tricalcium silicate at different mixtures. The tricalcium:dicalcium silicate ratio of approximately 0.85 was observed to have a higher rate of formation of products, the appearance of more permeable C−S−H, and ultimately more product. Initial compressive strength testing indicated that these reaction mechanics lead to an optimum in the strength at this composition ratio. Interestingly, this ratio of components is close to the ratios commonly used in industrial clinkers. These results demonstrate that the overall hydration reaction cannot be simply described as a linear combination of the reactions for the individual components. In particular we have observed anomalies in most of the kinetic parameters at composition ranges of $x = 0.75$ to 0.90.

Acknowledgment. Thanks to Dr. Craig Brown from the NIST Center for Neutron Research for help with QENS data collection. Thanks to Dr. Chiara (Clarissa) Ferraris of NIST for help with compressive strength testing. We acknowledge the support of NIST, U.S. Department of Commerce, in providing the neutron research facilities used in this work. Manufacturers are identified to provide complete identification of experimental conditions, and such identification is not intended as a recommendation by the University of Maryland, NIST, or the Federal Highway Administration.

References and Notes

(1) Tong, H. S.; Young, J. F. *J. Am. Ceram. Soc.* **1977**, *60*, 321.
(2) Odler, I.; Schüppstuhl, J. J. *Cem. Concr. Res.* **1982**, *12*, 13.
(3) Taylor, H. F. W. *Cement Chemistry*, 2nd ed.; Thomas Telford: London, UK, 1997.
(4) Allen, A. J.; McLaughlin, J. C.; Neumann, D. A.; Livingston, R. A. *J. Mater. Res.* **2004**, *19*, 3242.
(5) FitzGerald, S. A.; Thomas, J. J.; Neumann, D. A.; Livingston, R. A. *Cem. Concr. Res.* **2002**, *32*, 409.
(6) Fratini, E.; Chen, S.-H.; Baglioni, P.; Bellissent-Funel, M. *Phys. Rev. E* **2001**, *64*, Art. No. 020201.
(7) Thomas, J. J.; FitzGerald, S. A.; Neumann, D. A.; Livingston, R. A. *J. Am. Ceram. Soc.* **2001**, *84*, 1811.
(8) FitzGerald, S. A.; Neumann, D. A.; Rush, J. J.; Bentz, D. P.; Livingston, R. A. *Chem. Mater.* **1998**, *10*, 397.
(9) *ASTM, Annual book of ASTM standards, section four*: *construction, designation*: *C 109/C*; ASTM: Philadelphia, PA, 2000.
(10) Copley, J. R.; Udovic, T. J. *J. Res. Natl. Inst. Stand. Technol.* **1993**, *98*, 71.
(11) DAVE, National Institute of Standards and Technology Center for Neutron Research.
(12) Thomas, J. J.; Jennings, H. M. *Chem. Mater.* **1999**, *11*, 1907.
(13) Thomas, J. J.; Chen, J. J.; Allen, A. J.; Jennings, H. M. *Cem. Concr. Res.* **2004**, *34*, 2297.